A Novel Route for Electrolytic Production of Very Branchy Copper Dendrites under Extreme Conditions

A Novel Route for Electrolytic Production of Very Branchy Copper Dendrites under Extreme Conditions

Journal:	*Journal of The Electrochemical Society*
Manuscript ID	JES-103351.R2
Manuscript Type:	Research Paper
Date Submitted by the Author:	15-Mar-2021
Complete List of Authors:	KARIMI TABAR SHAFIEI, FATEMEH; Malek-Ashtar University of Technology, Faculty of Material & Manufacturing Technologies Jafarzadeh, Kourosh; Malek-Ashtar University of Technology, Faculty of Material & Manufacturing Technologies Madram, Alireza; Malek-Ashtar University of Technology, Faculty of Chemical Engineering Nikolic, Nebojsa; University of Belgrade,
Keywords:	copper, chloride, the pulsating overpotential (PO) regime, dendrite, scanning electron microscope

A Novel Route for Electrolytic Production of Very Branchy Copper Dendrites under Extreme Conditions

Fatemeh Karimi Tabar Shafiei,[1] Kourosh Jafarzadeh,[1,z] Ali Reza Madram,[2] and Nebojša D. Nikolić[3]

[1]Faculty of Material & Manufacturing Technologies, Malek Ashtar University of Technology, Tehran, Iran

[2] Faculty of Chemical Engineering, Malek Ashtar University of Technology, Tehran, Iran

[3]University of Belgrade, Institute of Chemistry, Technology and Metallurgy, Department of Electrochemistry, Belgrade, Serbia

[z]E-mail: kjafarzadeh@mut.ac.ir

Abstract

Copper electrodeposition in a form of powder was examined using the pulsating overpotential (PO) regime from the sulfate electrolyte without or with an addition of various concentrations of chloride ions. Morphological and structural characteristics of the produced particles were analyzed by the scanning electron microscope (SEM) and the X-ray diffraction (XRD) method. The final morphology of Cu powders was determined with two parallel processes: a) suppression of hydrogen evolution reaction due to pause duration considerably longer than the deposition time, and b) catalytic effect of added chlorides. Depending on the amplitude of overpotential applied, addition of chlorides into the solution led to either an appearing of dendrites or to formation of very branchy dendrites, what confirms a catalytic effect of these ions on the process of Cu electrolysis. The novel forms of copper dendrites, such as the needle-like and the 2D (two dimensional), were identified in this investigation, and the catalytic effect of chlorides on copper electrodeposition has been just discussed by morphological analysis of these dendritic forms. The XRD analysis of the copper dendrites obtained with an addition of chlorides showed predominantly oriented the Cu crystallites in (111) plane.

Introduction

Copper powder market is one of the largest growing market in the world, with an estimated growth of almost 500 milion USD during 2020 – 2026 [1]. This growth is caused by the fact that almost all industrial branches are consumers of copper powder. Application of copper powder is primarily based on its high electrical and thermal conductivity, making this powder very suitable in fabrication of electronic and electrical parts [2]. Due to use in pharmaceuticals, biochemical sector is also large consumer of this powder. Aside from the electronic and pharmaceutical industries, the other large consumers are powder metallurgy sector, industrial machinery manufacturing, production of coating and conductive inks,

alloyed with other metals like zinc, tin, nickel for decorative paintings and coatings, in manufacturing printing inks, antifouling paints, etc [2].

Application of Cu powder in all above-mentioned technologies is associated with a size and form of particles. Cu powder consists of particles of various size from a nano scale to those of several hundred microns [3]. The shape of particles is determined by a way of their production, and irregular rough, spherical, dendritic and cauliflower-like are a typical forms of Cu particles [4]. Irrespective of method production, the demands which Cu powder must fulfill for various applications are high purity, without or with low content of oxygen, low-temperature sintering activity, etc. For that purpose, to avoid oxidation of Cu powder the process of its stabilization with compounds like benzoic acid and K – Na tartarate is often used [5].

The main ways for production of Cu as powder are: the ultrasonic spray pyrolysis [6], hydrometallurgy [7], water and gas atomization [8, 9], gel-casting [10], chemical reduction methods [11], electrolysis [3, 12–19], etc. The spherical form of the particles is usually obtained by the ultrasonic spray pyrolysis and gas atomization, irregular particles are formed by water atomization, while dendritic and cauliflower-like particles are the most often forms obtained by electrolysis. Electrolysis is often used way for a production of Cu powder, with many advantages relative to the other synthesis methods. These advantages can be summarized as follows: easy control of size and form of particles by the selection of the working conditions and regimes of electrodeposition, a low equipment and product cost, a high purity of the produced particles, environmentally friendly, low energy consumption, etc. [20].

The electrolytic obtained dendrites of Cu are 3D (three dimensional) form like a tree of pine and are constructed from the corncob-like parts representing its basic element [3, 12]. They are formed without or with negligible contribution of evolved hydrogen as the second reaction in the powder production range. The cauliflower-like forms represent the other type of particles obtained by electrolysis and they are formed under strong effect of parallel hydrogen evolution reaction [3, 12]. The micro structure of both dendritic and cauliflower-like particles was similar and consisted of agglomerates of approximately spherical grains. Copper as powder can be obtained by all available electrolysis techniques including both the constant [3, 12–19] and pulse reverse [3, 15, 21–23] regimes of electrolysis. The main parameters determining the particle size and distribution are: the type and composition of electrolyte, temperature, the type of working electrode, circulation rate, a design of experments, etc. [3, 24–27]. In the last time, a special attention is devoted to the effect of various addition agents or additives added to the electrolyte on mophology, size and distribution of the Cu particles [21, 28–32]. The some typical additives used in the processes of Cu electrolysis are: polyvinylpyrrolidone (PVP) [21, 30], sodium dodecyl sulfate (SDS) [21, 30, 32], polyethylene glycol (PEG) [21], cellulose [21], cetyltrimethylammonium bromide (CTAB) [30, 32–35], thiourea (Tu) [21], potassium ferrocyanide [29] and 2,2′-dipyridine [29], etc. For example, the particles of spherical shape can be obtained by addition of the mixture of potassium ferrocyanide and 2,2′-dipyridine.

An chloride ions are widely used as additive in Cu electrodeposition processes from the sulfate electrolytes, and the effect of this additive on mechanism of Cu electrodeposition is well elaborated [36–38]. However, the effect of chloride ions on dendritic growth has not

been enough explored, and the only few data can be found in the literature [39, 40]. On the other hand, pulse reverse regimes of electrolysis, like pulsating overpotential (PO) [41, 42], offer a great possibility in investigation of metal electrodeposition processes, because deposits of desired characteristics can be obtained by an easy regulation of parameters constructing these regimes. Combining benefits which can be achieved by application of both chloride ions as additive and pulse reverse regimes on a quality of metal deposits, the aim of this investigation was to analyze an influence of various concentrations of chloride ions added to the basic sulfate electrolyte on formation of Cu dendrites by use of the PO regime. The novel procedure predicting a formation of Cu dendrites in conditions in which their formation was not possible by application of constant regimes of electrodeposition will be proposed. It will be done by application of very long pause duration, the very high overpotential amplitudes and by addition of chloride ions.

Experimental

The square-wave pulsating overpotential (PO) regime consisted of 30 ms long pulse of deposition (t_c) and 100 ms long pause duration (t_p) was used for copper electrodeposition. The selected overpotential amplitudes (η_A) were: –1100, –1250 and –1400 mV vs. Ag/AgCl. Electrodeposition of Cu was performed from the sulfate electrolyte (0.15 M $CuSO_4$ + 0.50 M H_2SO_4), without or with 5, 15 and 30 mM added HCl. The solution was prepared using the high purity water (Milipore, 18 MΩ cm) and p.a. reagents. The cathodic polarization curves for electrodeposition of copper from the same solutions were recorded potentiostatically in the potential range of zero to –1500 mV with a scan rate of 5 mV/s. The Tafel plots were obtained in the potential range of OCP ± 250 mV with a scan rate of 0.001 V/s. The cathodic Tafel slopes were plotted versus different chloride ion concentrations.

All electrochemical experiments were performed at a temperature of 22.0 ± 0.50 ^oC in a three-electrode cell using potentiostat/galvanostat Autolab (GTSTAT101) with GPES software Version 4.5. In all experiments, an electrodeposition time was 480 s. The working electrode was the high purity copper (99.8 %), while the counter and the reference electrodes were a Pt grid and Ag/AgCl (3 M KCl), respectively.

For morphological characterization of electroltically obtained Cu deposits, a scanning electron microscope (SEM), model TESCAN Digital Microscopy, VEGA3 was used. The selected Cu deposit chemical composition was analyzed by X-ray energy dispersive spectroscopy (EDS), model Oxford, UK INCA X-MAX. Crystallographic structures determination was performed by X-ray diffraction (XRD) with a diffractometer model Philips PW1730 and a monochromatic Cu Kα radiation (λ = 0.15405 nm). The peaks were identified in comparison with the Joint Committee on Powder Diffraction Standards (JCPDS) files.

Results and discussion

Figure 1 shows copper powder deposits produced from an electrolyte containing 0.15 M $CuSO_4$ in 0.50 M H_2SO_4 by the PO regimes with η_A of –1100 mV (Figure 1a and 1b), –1250 mV (Figure 1c and 1d) and –1400 mV (Figure 1e and 1f). The PO regimes with t_c of 30 ms and t_p of 100 ms were applied in all experiments. The small agglomerates of Cu grains of cauliflower-like shape were obtained with η_A of –1100 mV (Figure 1a and 1b). Aside from these Cu grains agglomerates (Figure 1c), an increase of η_A from –1100 to –1250 mV led to

formation of three-dimensional (3D) dendritic forms, as shown on Figure 1d. The similar morphological forms were also observed with η_A of –1400 mV. The mixture of cauliflower-like agglomerates of Cu grains and 3D dendritic particles was obtained with this amplitude of overpotential (Figure 1e and 1f).

Applying the same PO regime, it is examined the influence of chloride ions on a shape of powdered particles, and the Cu deposits obtained with different concentrations of added chlorides are shown on Figures 2–4.

Figure 2 shows the Cu powder deposits obtained with η_A of –1100 mV and concentrations of chloride ions of 5 mM (Figure 2a and 2b), 15 mM (Figure 2c and 2d) and 30 mM (Figure 2e and 2f). Formation of dendritic forms with appearing those in the form of needles occurs with the smallest concentration of added chlorides (Figure 2a and 2b). The addition of chloride ions in a concentration of 15 mM led to a formation of branched dendrites including formation and those in the form of needles (Figure 2c and 2d). Finally, the dendrites with the sharp tips, and well defined trunk and branches are predominantly formed with the largest examined concentration of chloride ions of 30 mM (Figure 2e and 2f). These dendrites have mainly the two dimensional (2D) shape.

The very branchy particles of dendritic shape were also obtained using η_A of –1250 mV (Figure 3). The dendrites formed with an addition of chloride ions in a concentration of 5 and 15 mM were mainly of the 3D shape (Figure 3a–3d). The presence of dendrites like needles can be also noticed among those obtained with a concentration of chloride ions of 15 mM (Figure 3c). At the end, the dendrites obtained with an addition of 30 mM HCl were predominantly 2D shape (Figure 3e and 3f).

Finally, the same trend in the shape of dendrites is kept with the largest analysed η_A of –1400 mV (Figure 4). The appearing of the needle-like dendrites as a result of addition of 5 mM chloride ions is also mentioned (Figure 4a and 4b). The very branchy 3D pine-like dendrites are formed with an addition of 15 mM chloride ions (Figure 4c and 4d). Finally, the dendrites like 2D are formed with 30 mM concentration of chloride ions (Figure 4e and 4f).

For the basic solution (0.15 M $CuSO_4$ + 0.50 M H_2SO_4), overpotential amplitudes of –1100, –1250 and –1400 mV are outside the limiting diffusion current density plateau and situated deep in the hydrogen evolution region [3, 43, 44] (see the polarization curve for Cu electrodeposition from the basic sulfate solution on Fig. 5a). The beginning of evolution of hydrogen as the parallel reaction to copper electrolysis corresponds to certain overpotential inside the limiting diffusion current density plateau, with a tendency of intensification of this reaction with an increase of overpotential. The starting from some overpotential, hydrogen evolution becomes so intensive that a strong influence on hydrodynamic conditions in the near-electrode layer is achieved, and it is manifested by the fast growth of the current density with further increase of overpotential at the polarization curve. In constant potentiostatic regime, the 3D pine-like dendrites are obtained under the diffusion control, inside the limiting diffusion current density plateau, while the cauliflower-like agglomerates of Cu grains are obtained at overpotentials outside the limiting diffusion current density plateau in conditions of vigorous hydrogen evolution [3, 43]. The cauliflower-like agglomerates of Cu grains were situated around holes formed by a detachment of hydrogen bubbles, making the typical 3D foam or the honeycomb-like structures.

The two parallel processes are responsible for morphological forms given on Figures 1–4:

(a) suppression of evolution of hydrogen as the second reaction, and (b) the strong effect of chloride ions on formation and growth of dendrites. Since hydrogen evolution reaction was completely suppressed, the current efficiency for copper electrodeposition reaction is 100 %. It is confirmed by the absence of holes originating from the detached hydrogen bubbles in the surface morphologies obtained under various electrodeposition conditions.

In our case, the evolution of hydrogen was completely suppressed by use of the PO regimes of long both pulse of deposition and pause, whereby pause duration was 3.33 longer than deposition pulse duration. In the PO regimes, morphology of metal deposits does not depend only on η_A and p (where p represents the pause to pulse ratio, and is defined as $p = t_p/t_c$), but also depends on the lengths of t_p and t_c for the same ratio [3]. With the applied overpotential amplitude in hydrogen evolution range, the increasing p leads to a decreasing amount of generated hydrogen with a strong consequences on the shape, size and distribution of holes formed by the detachment of hydrogen bubbles [15]. Simultaneously, the change of morphology of Cu deposits around holes from an agglomerates of Cu grains of cauliflower-like shape to very branchy dendritic particles was noticed. At p values considerably larger than 1, evolution of hydrogen can be completely inhibited, and various structures like pyramid-like are formed [3].

By the selection of the suitable η_A and p values in the PO regime, morphology of metal deposit becomes similar to that formed under the constant potentiostatic conditions (p = 0) at an overpotential of electrodeposition lower than that corresponding to the applied amplitude of overpotential [3]. The increasing p values lead to decreasing the degree of diffusion control, and deposits corresponding to the activation, or the activation-diffusion control can be obtained. In our case, depending on the overpotential amplitude applied, the copper deposits obtained in the absence of chloride ions (Figure 1) correspond to those formed at overpotentials inside the diffusion controlled electrodeposition. In the constant potentiostatic regime, the cauliflower-like agglomerates of Cu grains (Figure 1a and 1b) are a feature of electrodeposition process at the overpotential belonging to very beginning of the full diffusion control before the dendritic growth was initiated. The appearing of mixture of Cu grains agglomerates of cauliflower-like shape and individual dendrites corresponds to the diffusion controlled electrodeposition under the constant potentiostatic conditions, but after the minimal overpotential for initiation of the dendritic growth was reached (Figure 1c–1f).

Anyway, the applied PO regime made the strong effect on morphology of Cu deposits by an inhibition of hydrogen evolution. On the other side, the addition of chloride ions to the electrolyte catalyzed or accelarated copper electrodeposition reaction [36]. In our case, it is manifested by either an appearing of dendrites at the overpotential amplitude of –1100 mV at which they are not formed from the electrolyte without added chlorides (Figure 2) or a strong ramification of already formed dendrites at higher overpotential amplitudes of –1250 and –1400 mV (Figures 3 and 4).

The cathodic polarization curves for Cu electrodeposition from the electrolytes with an addition of 5, 15 and 30 mM HCl are also shown on Fig. 5a. The addition of chloride ions caused a depolarization of the electrode potential (see inset on Fig. 5a) and the decrease of the limiting diffusion current density values without any effect on length of the plateaus. Simultaneously, aside from on the values of the current density peak, there was no any other significant effect of various concentrations of chloride ions on the polarization characteristics

of copper. The increase of the maximum current density with increasing the concentration of chloride ions, together with the depolarization on the beginning of deposition process reveals a catalytic effect of chloride on Cu electrodeposition, and it was in an accordance with those found in Ref. [38]. The limiting diffusion current densities for the electrolytes with the chlorides were for about 25 % smaller than the value obtained for the basic sulfate electrolyte.

The catalytic effect of chloride ions can be ascribed to formation of adsorbed chloride layer at the electrode surface which mediates to a reduction of Cu(II) ions introducing an additional reaction pathways in a mechanism of Cu electrodeposition [40]. Namely, electrodeposition of Cu from chloride free acid sulfate electrolytes occurs through two successive one-electron reactions [40]:

$$Cu^{2+} + e^- = Cu^+ \qquad E° = -0.087\ V_{SCE} \qquad (1)$$

and

$$Cu^+ + e^- = Cu \qquad E° = 0.281\ V_{SCE} \qquad (2)$$

where a reaction path (1) is the rate-determining step.

When chloride ions were added, the two additional reaction steps occur parallelly with reaction steps (1) and (2) [40]:

$$Cu^{2+} + Cl^-_{ads} + e^- = CuCl_{ads} \qquad E° = 0.338\ V_{SCE} \qquad (3)$$

and

$$CuCl_{ads} + e^- = Cu + Cl^- \qquad E° = -0.063\ V_{SCE} \qquad (4)$$

These competitive reaction pathways cause an acceleration of Cu electrodeposition process and formation of very branchy dendrites. This mechanism predicting adsorption of chloride ions at the cathode results in an overall depolarization of process of reduction and it is valid for concentrations of chloride ions in the electrolytes up to 100 mM [40], that was the case in this investigation.

Simultaneously, the catalytic effect of added chlorides on Cu electrodeposition can be explained by ab inito molecular orbital theory [37], by which small concentrations of chloride ions added to the solution change mechanism of reaction for electron transfer from an outer-sphere reaction (water–water bridge) to an inner-sphere reaction (chloride bridge) what results in an increase of the exchange current density (i_0) for Cu^{2+}/Cu^+ reaction step [37].

The dependencies of the cathodic Tafel slopes on a concentration of the chloride ions are shown on Fig. 5b. The values of Tafel slope in the 116 – 140 mV dec^{-1} range indicate that the reduction process occurs mostly through the two consecutive one-electron reactions (Eqs. (1) and (2)), and which is slightly effected by the presence of adsorbed complex Cu–Cl [38, 40].

The catalytic effect of chloride ions can be confirmed by a shape of dendrites formed with added chlorides. Some of shapes of Cu dendrites like the needle-like (Figures 2b, 3c and 4b) and those of the 2D shape (Figures 2f, 3f and 4f) substantially differ from the usual referred shape for the Cu dendrite. As already mentioned, the typical Cu dendrite is 3D (three dimensional) pine-like shape with stalk and branches in the corncob-like form [3, 12]. The needle-like and very long 2D dendrites are a feature of processes of the electrodeposition characterized by the higher i_0 values than that for Cu [45], such as Ag [46] and Zn [47].

Figure 6 shows the dependencies of the particle size defined by a length of dendrite stalk on the concentration of chloride ions obtained at the given overpotential amplitudes. The largest effect is achieved with the largest analysed concentartion of chloride ions of 30 mM. The 2D dendrites were predominantly formed with this concentration of chlorides (Figures 2–4).

Irrespective of the shape of the dendrite, all forms of Cu dendrites shown here follow both the electrochemical [3, 47] and classical Wranglen's [48] definition of dendrite. Regarding an electrochemical definition, a dendrite represents an irregularity or protrusion created in the initial stage of process of the electrodeposition and burried deep in the diffusion layer of macroelectrode. The spherical diffusion layer is formed around the tip of protrusion, causing the activation controlled growth of such tip. Simultaneously, the electrodeposition process on an electrode surface is the full diffusion controlled [3].

Wranglen defines a dendrite as a sceleton consisted from stalk and branches giving to a dendrite an appearance of tree [48]. The 2D dendrite represents a dendrite which stalk and branches are in the one plane. The branches developed from a stalk are denoted by primary branches, while the corresponding dendrite is denoted as primary (P) dendrite. The secondary branches are developed from primary branches, while such dendrite is referred as secondary (S) dendrite. Hence, some of the Cu dendrites obtained in the presence of chlorides (Figures 2e and 2f, 3e and 3f, 4e and 4f) belong to S type. Simultaneously, the very branchy 3D dendrites with the sharp tips and consisted of small approximately spherical grains were also formed. They keep the pine-like shape (Figures 3b and 3d), but were considerably smaller than the usual referred 3D pine-like Cu dendrite.

The catalytic effect of chloride ions can be also perceived as follows: without chloride ions, an obtaining of the individual dendrites with overpotential amplitudes of –1250 and –1400 mV (Figure 1c–1f) indicated that the critical overpotential for initiation of growth of dendrite, η_i [3] was reached with these overpotential amplitudes. On the other hand, this overpotential was not reached with η_A of –1100 mV (Figure 1a and 1b). Formation of branchy dendrites as only surface morphology from the electrolytes containing chloride ions (Figures 2–4) clearly indicates that the critical overpotential for instantaneous growth of dendrite, η_c [3] was exceeded with all three ovepotential amplitudes, that represents a clear proof of the strong acceleration of the electrodeposition processes with added chloride ions.

The EDS spectrums obtained from the parts of Cu dendrites close to their tips, together with the corresponding SEM micrograph, are shown on Figure 7. EDS analysis showed only the presence of copper, while the presence of chlorine was not detected in the Cu dendrites. This was in accordance with previosly reported investigations [39, 49] that in the electrolytes with a concentration of chloride ions smaller than 50 mM, all chlorine is dissolved at cathodic overvoltage higher than 146 mV (vs. Cu/Cu^{2+}); the condition fulfilled in our case.

Figure 8 displays the X-Ray diffractogram of the Cu dendrites formed with η_A of –1250 mV using a concentration of chloride ions of 5 mM. Three diffraction peaks by orientations along the (111), (200) and (220) directions correspond to 2θ angles of 43.3˚, 50.5˚ and 74.2˚ are indexed according to the face centered cubic (FCC) copper structure as indicated in reference code (04-0386).

The diffraction peaks that would indicate on the presence of impurities such as copper oxide or copper hydroxide are not detected, meaning that the obtained Cu powders were of the high purity. This result is consistent with that of EDS analysis.

The sharp and strong peaks showed that the produced particles of Cu were very crystalline. It is well known that crystal facets that grow more slowly exhibit stronger intensity in the XRD pattern and consequently found more on the surface of the crystal. Therefore, it can be concluded that because the surface energy of (111) plane in FCC crystal lattice is lower than the other planes like (200) and (220), respectively, the dendritic Cu is abundant in {111} planes [50]. Due to the difference in surface energy of different crystal planes, the rate of electrodeposition on each of them is different. In other words, the rate of crystal growth onto Cu crystal planes is as follows: (220) > (200) > (111) [51]. The Cu crystallites oriented in (111) plane are the origin from the growth centers present in the interior of the Cu crystals. The (111) plane is denoted as slow growing plane, and this crystal plane survives in the growth process, causing the predominant orientation of Cu crystallites in this plane in all dendritic shapes. The other planes such as (220) and (200) belong to the fast growing planes, and they disappear through the growing process. The origin of Cu crystallites oriented in these planes is primarily of growth centers present at the tips of growing crystals, and hence, the tips of all dendritic shapes are constructed from them [17]. Anyway, for the difference from morphology of the particles, the addition of chloride ions does not affect their crystalographic charactecteristics. The Cu crystallites remained predominatly oriented in the (111) plane as already observed in the dendritic particles obtained without an addition of the chloride ions [17].

Finally, the 2D shape of the Cu dendrite was very similar to the Cu dendrites obtained by a galvanic replacement reaction (GRR)-based solution chemistry methodology [52]. According to this method of synthesis of Cu dendrites, Cu was obtained on gold foil in the presence of added chloride ions as HCl or NaCl, where chloride ions augment an uninterrupted replacement reaction. This similarity can indicates the strong correlation between the form of Cu dendrites and an addition of chloride ions irrespective of method of their synthesis. Certainly, it will be the subject of the future investigation.

Anyway, a novel procedure for a production of very branchy Cu dendrites by the PO regime is proposed. The superfine dendrites constructed from small approximately spherical grains, as well as the needle-like and the 2D dendrites were formed in conditions in which their formation was not possible in the constant potentiostatic regime. It is attained by application of the high overpotential amplitudes, enough long pause duration to suppress hydrogen evolution reaction, and by the catalytic effect of the chloride ions.

Conclusions

Influence of chloride ions on formation and shape of Cu dendrites produced by the PO regime has been investigated by the SEM analysis of the obtained powders. The sulfate electrolyte containing 0.15 M $CuSO_4$ in 0.50 M H_2SO_4 without or with an addition of 5, 15 and 30 mM HCl was used in this investigation. In all PO regimes, a t_c of 30 ms and a t_p of 100 ms are used, while the values of overpotential amplitude were varied to be –1100, –1250 and –1400 mV vs. Ag/AgCl. It can be concluded from the obtained results:

1. Dependeng on the overpotential amplitude applied, the application of PO regime with the pause duration 3.33 times longer than the deposition pulse led to a suppression of

evolution of hydrogen as a parallel reaction, causing formation of either caulflower-like structures or individual dendrites.

2. The addition of chloride ions catalyzes Cu electrodeposition reaction, that is manifested by a formation of very branchy dendrites, as well as by their appearing at the overpotential amplitude at which they are not formed without added chloride ions.
3. The some novel forms of Cu dendrites like the needles and the 2D forms were identified in this investigation.
4. In the dendritic particles prepared from the electrolyte with an addition of chloride ions, the crystallites of Cu were predominantly oriented in (111) plane.

References

[1]https://www.marketwatch.com/press-release/copper-powder-market-size-forecast-period-of-2020-to-2025-detailed-investigation-of-global-market-size-regional-and-country-level-market-top-companies-industry-outlook-2020-10-04.

[2] https://www.transparencymarketresearch.com/copper-copper-alloy-powder-market.html.

[3] K. I. Popov, S. S. Djokić, N. D. Nikolić and V. D. Jović, Morphology of electrochemically and chemically deposited metals, Springer, New York, NY, USA, 2016, pp. 1–368. https://doi.org/10.1007/978-3-319-26073-0.

[4] Lj. Avramović, V. M. Maksimović, Z. Baščarević, N. Ignjatović, M. Bugarin, R. Marković and N. D. Nikolić, Influence of the shape of copper powder particles on the crystal structure and some decisive characteristics of the metal powders, *Metals*, **9** 56 (2019). https://doi.org/10.3390/met9010056.

[5] M. G. Pavlović, Lj. J. Pavlović, I. D. Doroslovački and N. D. Nikolić, The effect of benzoic acid on the corrosion and stabilisation of electrodeposited copper powder, *Hydrometallurgy*, **73**, 155 (2004). https://doi.org/10.1016/j.hydromet.2003.08.005.

[6] S. Stopić, P. Dvorak and B. Friedrich, Synthesis of spherical nanosized copper powder by ultrasonic spray pyrolysis, *World of Metallurgy – ERZMETALL*, **58**, 195 (2005). https://doi.org/10.1016/j.materresbull.2006.03.006.

[7] S. S. Djokić, Production of metallic powders from aqueous solutions without an external current source, in: S. S. Djokić (Eds), Electrochemical Production of Metal Powders, Series: Modern Aspects of Electrochemistry, Springer, New York, NY, USA, 2012, volume 54, pp. 369–398. https://link.springer.com/bookseries/6251.

[8] O. Neikov, S. Naboychenko, I. Mourachova, V. Gopienko, I. Frishberg and D. Lotsko, Production of copper and copper alloy powders, in Handbook of Non-Ferrous Metal Powders: Technologies and Applications, Elsevier, Oxford, United Kingdom, 2009, pp. 331–332. https://doi.org/10.1016/b978-1-85617-422-0.00016-1.

[9] https://www.copper-powder99.com/copper-powder/gas-atomized-copper-powder/.

[10] W. Chen, J. Cheng, H. Chen, N. Ye, B. Wei, L. Luo and Y. Wu, Nanosized copper powders prepared by gel-casting method and their application in lubricating oil, *Trans. Nonferrous Met. Soc. China*, **28**, 1186 (2018). https://doi.org/10.1016/s1003-6326(18)64756-9.

[11] M. S. Aguilar, R. Esparza and G. Rosas, Synthesis of Cu nanoparticles by chemical reduction method, *Trans. Nonferrous Met. Soc. China*, **20**, 1510 (2019). https://doi.org/10.1016/s1003-6326(19)65058-2.

[12] N. D. Nikolić, Lj. J. Pavlović, M. G. Pavlović and K. I. Popov, Morphologies of electrochemically formed copper powder particles and their dependence on the quantity of evolved hydrogen, *Powder Technol.*, **185**, 195 (2008). https://doi.org/10.1016/j.powtec.2007.10.014.

[13] G. Orhan and G. Hapci, Effect of electrolysis parameters on the morphologies of copper powder obtained in a rotating cylinder electrode cell, *Powder Technol.*, **201**, 57 (2010). https://doi.org/10.1016/j.powtec.2010.03.003.

[14] G. Orhan and G. G. Gezgin, Effect of electrolysis parameters on the morphologies of copper powder obtained at high current densities, *J. Serb. Chem. Soc.*, **77**, 651 (2012). https://doi.org/10.2298/jsc110627196o.

[15] N. D. Nikolić, G. Branković and M. G. Pavlović, Correlate between morphology of powder particles obtained by the different regimes of electrolysis and the quantity of evolved hydrogen, *Powder Technol.*, **221**, 271 (2012). https://doi.org/10.1016/j.powtec.2012.01.014.

[16] T. N. Ostanina, V. M. Rudoi, A. V. Patrushev, A. B. Darintseva and A. S. Farlenkov, Modelling the dynamic growth of copper and zinc dendritic deposits under the galvanostatic electrolysis conditions, *J. Electroanal. Chem.*, **750**, 9 (2015). https://doi.org/10.1016/j.jelechem.2015.04.031.

[17] N. D. Nikolić, Lj. Avramović, E. R. Ivanović, V. M. Maksimović, Z. Baščarević and N. Ignjatović, Comparative morphological and crystallographic analysis of copper powders obtained under different electrolysis conditions, *Trans. Nonferrous Met. Soc. China*, **29**, 1275 (2019). https://doi.org/10.1016/s1003-6326(19)65034-x.

[18] N. D. Nikolić, P. M. Živković, M. G. Pavlović and Z. Baščarević, Overpotential controls a morphology of electrolytically produced copper dendritic forms, *J. Serb. Chem. Soc.*, **84**, 1209 (2019). https://doi.org/10.2298/jsc190522066n.

[19] V. S. Nikitin, T. N. Ostanina, V. M. Rudoi, T. S. Kuloshvili and A. B. Darintseva, Features of hydrogen evolution during electrodeposition of loose deposits of copper, nickel and zinc, *J. Electroanal. Chem.*, **870**, 114230 (2020). https://doi.org/10.1016/j.jelechem.2020.114230.

[20] M. Amiri, S. Nouhi and Y. Azizian-Kalandaragh, Facile synthesis of silver nanostructures by using various deposition potential and time: A nonenzymetic sensor for hydrogen, *Mater. Chem. Phys.*, **155**, 129 (2015). https://doi.org/10.1016/j.matchemphys.2015.02.009.

[21] R. K. Nekouei, F. Rashchi and N. N. Joda, Effect of organic additives on synthesis of copper nano powders by pulsing electrolysis, *Powder Technol.*, **237**, 554 (2013). https://doi.org/10.1016/j.powtec.2012.12.046.

[22] K. I. Popov, Lj. J. Pavlović, E. R. Ivanović, V. Radmilović and M. G. Pavlović, The

effect of reversing current deposition on the apparent density of electrolytic copper powder, *J. Serb. Chem. Soc.*, **67**, 61 (2002). https://doi.org/10.2298/jsc0201061p.

[23] S. Wahyudi, S. Soepriyanto and M. Z. Mubarok, Sutarno, Effect of pulse parameters on the particle size of copper powder electrodeposition, *IOP Conf. Ser. Mater. Sci. Eng.*, **547**, 012020 (2019). https://doi.org/10.1088/1757-899x/547/1/012020.

[24] M. G. Pavlović, Lj. J. Pavlović, V. M. Maksimović, N. D. Nikolić and K. I. Popov, Characterization and morphology of copper powder particles as a function of different electrolytic regimes, *Int. J. Electrochem. Sci*., **5**,1862 (2010).

[25] R. K. Nekouei, F. Rashchi and A. Ravanbakhsh, Copper nanopowder synthesis by electrolysis method in nitrate and sulfate solutions, *Powder Technol*., **250**, 91 (2013). https://doi.org/10.1016/j.powtec.2013.10.012.

[26] R. K. Nekouei, F. Rashchi and A. A. Amadeh, Using design of experiments in synthesis of ultra-fine copper particles by electrolysis, *Powder Technol*., **237**, 165 (2013). https://doi.org/10.1016/j.powtec.2013.01.032.

[27] H. Wang, Q. Wang, W. Xia, B. Ren, Effect of jet flow between electrodes on power consumption and the apparent density of electrolytic copper powders, *Powder Technol*., **343**, 607 (2019). https://doi.org/10.1016/j.powtec.2018.11.078.

[28] J. Xue, Q. Wu, Z. Wang and S. Yi, Function of additives in electrolytic preparation of copper powder, *Hydrometallurgy*, **82**, 154 (2006). http://dx.doi.org/10.1016/j.hydromet.2006.03.010.

[29] W. Lou, W. Cai, P. Li, J. Su, S. Zheng, Y. Zhang and W. Jin, Additives-assisted electrodeposition of fine spherical copper powder from sulfuric acid solution, *Powder Technol*., **326**, 84 (2018). https://doi.org/10.1016/j.powtec.2017.12.060.

[30] H. Dong, Y. Wang, F. Tao and L. Wang, Electrochemical fabrication of shape-controlled copper hierarchical structures assisted by surfactants, *J. Nanomater*., 901842 (2012). https://doi.org/10.1155/2012/901842.

[31] F. Pagnanelli, Shape evolution and effect of organic additives in the electrosynthesis of Cu nanostructures, *J. Solid State Electrochem*., **23**, 2723 (2019). https://doi.org/10.1007/s10008-019-04360-z.

[32] B. Nanda and M. Mallik, Production of copper powder by electrodeposition with different equilibrium crystal shape, *Trans. Indian Inst. Met*., **73**, 2113 (2020). https://doi.org/10.1007/s12666-020-02015-6.

[33] H. Wu, Z. Li, Y. Wang, X. Li and W. Zhu, Inhibition effect of CTAB on electrodeposition of Cu in micro via: experimental and MD simulation investigations. *J. Electrochem. Soc*., **166**, D816 (2019). https://doi.org/10.1149/2.0651915jes .

[34] H. Wu, Z. Li, Y. Wang and W. Zhu, Communication—fast bottom-up filling of high aspect ratio micro vias using a single CTAB additive, *J. Electrochem. Soc.*, **167**, 132507 (2020). https://doi.org/10.1149/1945-7111/abbce5 .

[35] H. Wu, Z. Li, Y. Wang, X. Li, F. Wang and W. Zhu, Experimental analysis of the co-deposition of metal Cu and nano-sized SiC particles with CTAB in micro via filling. *J. Electrochem. Soc*., **166**, D237 (2019). https://doi.org/10.1149/2.0771906jes .

[36] D. M. Soares, S. Wasle, K. G. Weil and K. Doblhofer, Copper ion reduction catalyzed by chloride ions, *J. Electroanal. Chem*., **532**, 353 (2002). https://doi.org/10.1016/s0022-0728(02)01050-1.

[37] Z. Nagy, J. P. Blaudeau, N. C. Hung, L. A. Curtis and D. J. Zurawski, Chloride ion catalysis of the copper deposition reaction, *J. Electrochem. Soc*., **142**, L87 (1995). https://doi.org/10.1149/1.2044254.

[38] W. Shao, G. Pattanaik and G. Zangari, Influence of chloride anions on the mechanism of copper electrodeposition from acidic sulfate electrolytes, *J. Electrochem. Soc*., **154**, D201 (2007). https://doi.org/10.1149/1.2434682.

[39] H. C. Shin, M. Liu, Copper foam structures with highly porous nanostructured walls, *Chem. Mater*., **16**, 5460 (2004). https://doi.org/10.1021/cm048887b.

[40] W. Shao and G. Zangari, Dendritic growth and morphology selection in copper electrodeposition from acidic sulfate solutions containing chlorides, *J. Phys. Chem. C*, **113**, 10097 (2009). https://doi.org/10.1021/jp8095456.

[41] T. N. Ostanina, V. M. Rudoy, V. S. Nikitin, A. B. Darintseva and S. L. Demakov, Change in the physical characteristics of the dendritic zinc deposits in the stationary and pulsating electrolysis, *J. Electroanal. Chem.*, **784**, 13 (2017). https://doi.org/10.1016/j.jelechem.2016.11.063.

[42] V. S. Nikitin, T. N. Ostanina and V. M. Rudoi, effect of parameters of pulsed potential mode on concentration changes in the bulk loose zinc deposit and its properties, *Russ. J. Electrochem.*, **54**, 665 (2018). https://doi.org/10.1134/S1023193518090070.

[43] N. D. Nikolić, K. I. Popov, Lj. J. Pavlović and M. G. Pavlović, The effect of hydrogen codeposition on the morphology of copper electrodeposits. I. The concept of effective overpotential, *J. Electroanal. Chem*., **588**, 88 (2006). https://doi.org/10.1016/j.jelechem.2005.12.006.

[44] F. K. T. Shafiei, K. Jafarzadeh and A. R. Madram, Copper deposits obtained by pulsating overpotential regime with a long pause and pulse duration from sulfated solutions, *J. Serb. Chem. Soc*., **85**, 795 (2020). https://doi.org/10.2298/jsc190712128s.

[45] N. D. Nikolić, Influence of the exchange current density and overpotential for hydrogen evolution reaction on the shape of electrolytically produced disperse forms, *J. Electrochem. Sci. Eng*., **10**, 111 (2020). https://doi.org/10.5599/jese.707.

[46] Lj. Avramović, E. R. Ivanović, V. M. Maksimović, M. M. Pavlović, M. Vuković, J. S. Stevanović and N. D. Nikolić, Correlation between crystal structure and morphology of potentiostatically electrodeposited silver dendritic nanostructures, *Trans. Nonferrous Met. Soc. China*, **28**, 1903 (2018). https://doi.org/10.1016/S1003-6326(18)64835-6.

[47] N. D. Nikolić, P. M. Živković, J. D. Lović and G. Branković, Application of the general theory of disperse deposits formation in an investigation of mechanism of zinc

electrodeposition from the alkaline electrolytes, *J. Electroanal. Chem*., **785**, 65 (2017). https://doi.org/10.1016/j.jelechem.2016.12.024.

[48] G. Wranglen, Dendrites and growth layers in the electrocrystallization of metals, *Electrochim. Acta*., **2**, 130 (1960). https://doi.org/10.1016/0013-4686(60)87010-7.

[49] M. Kang and A. A. Gewirth, Influence of additives on copper electrodeposition on physical vapor Deposited (PVD) Copper Substrates, *J. Electrochem. Soc*., **150**, C426 (2003). https://doi.org/10.1149/1.1572152.

[50] B. Luo and X. Li, 3D porous copper films with large specific surface prepared by hydrogen bubble template, *Asian. J. Chem*., **25**, 9927 (2013). https://doi.org/10.14233/ajchem.2013.15640.

[51] J. O' M. Bockris, A. K. N. Reddy, M. Gamboa-Aldeco, Modern Electrochemistry 2A, Fundamentals of Electrodics, Kluwer Academic/Plenum Publishers, New York, NY, USA, (2000), p. 1333.

[52] R. Bakthavatsalam, S. Ghosh, R. K. Biswas, A. Saxena, A. Raja, M. O. Thotiyl, S. Wadhai, A. G. Banpurkar and J. Kundu, Solution chemistry-based nano-structuring of copper dendrites for efficient use in catalysis and superhydrophobic surfaces, *RSC Adv*., **6**, 8416 (2016). https://doi.org/10.1039/c5ra22683j.

Figures

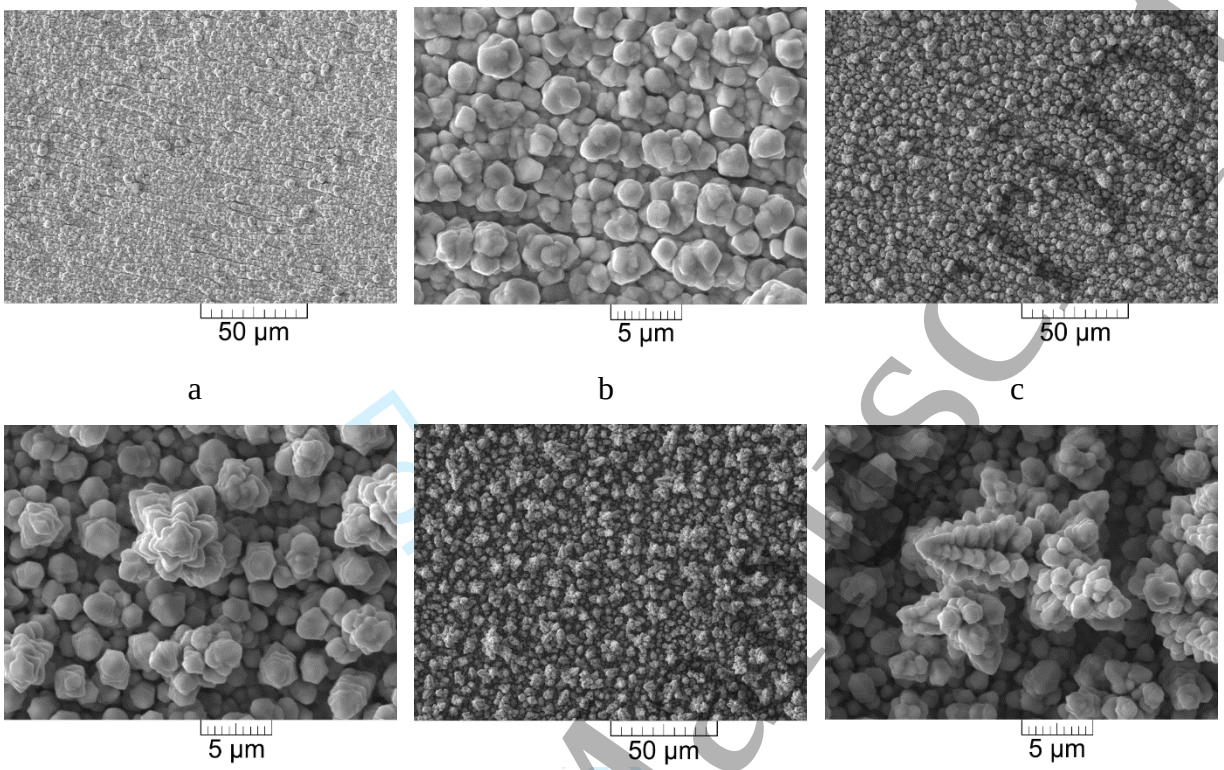

Figure 1. Morphologies of Cu deposits produced by the PO regime from 0.15 M $CuSO_4$ in 0.50 M H_2SO_4 with η_A of: a) and b) –1100 mV, c) and d) –1250 mV, and e) and f) –1400 mV.

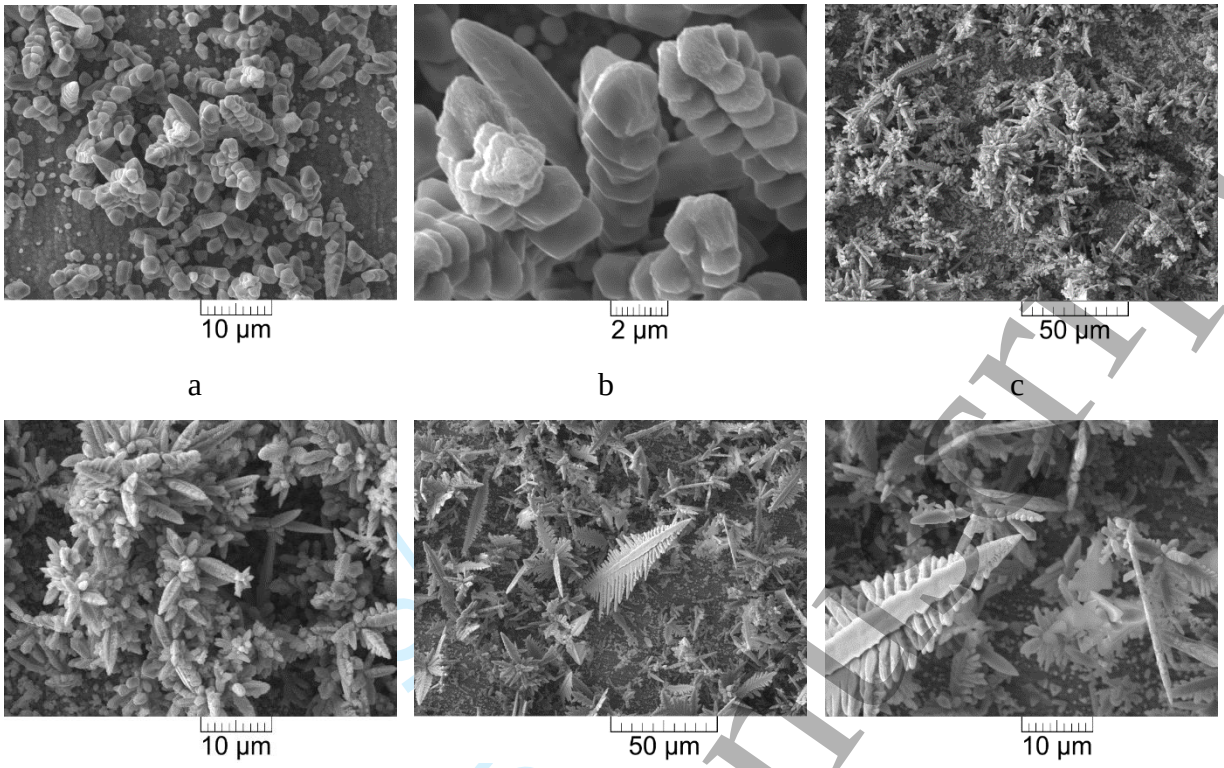

Figure 2. Morphologies of Cu deposits produced by the PO regime from 0.15 M $CuSO_4$ in 0.50 M H_2SO_4 with η_A of –1100 mV and by an addition of chloride ions of: a) and b) 5 mM, c) and d) 15 mM, and e) and f) 30 mM HCl.

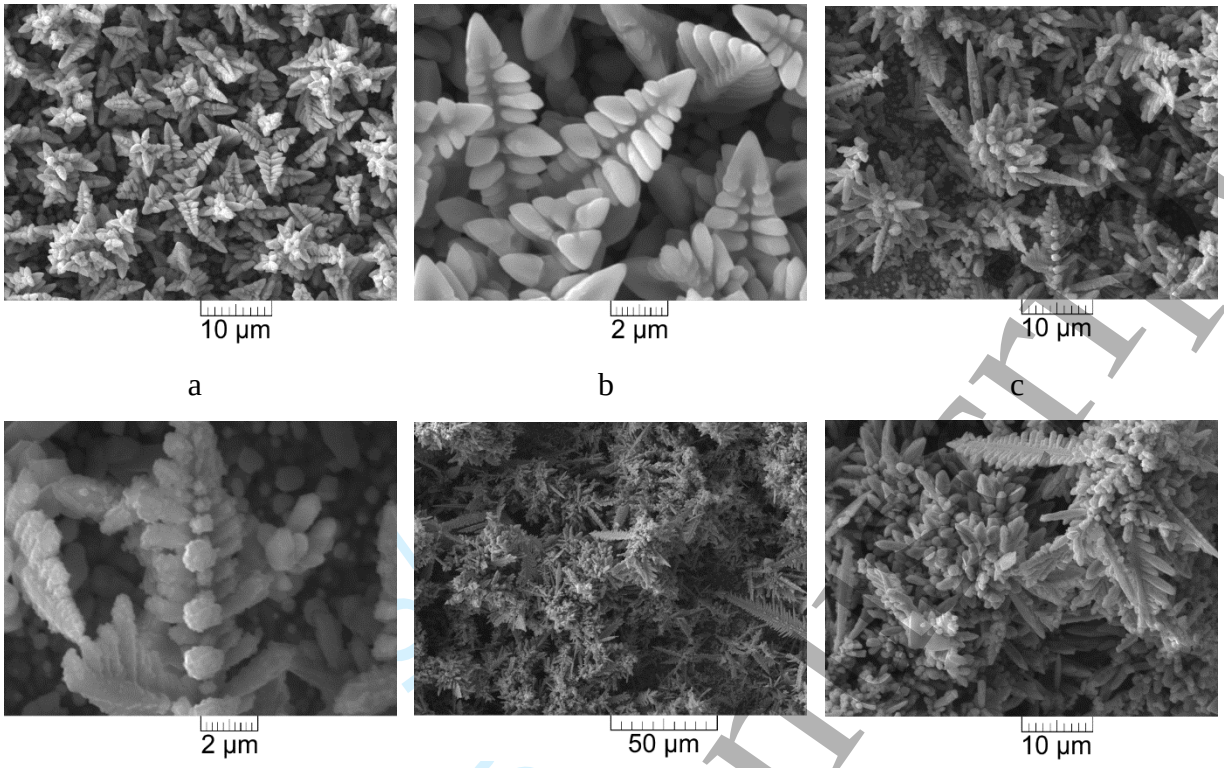

Figure 3. Morphologies of Cu deposits produced by the PO regime from 0.15 M $CuSO_4$ in 0.50 M H_2SO_4 with η_A of –1250 mV and by an addition of chloride ions of: a) and b) 5 mM, c) and d) 15 mM, and e) and f) 30 mM HCl.

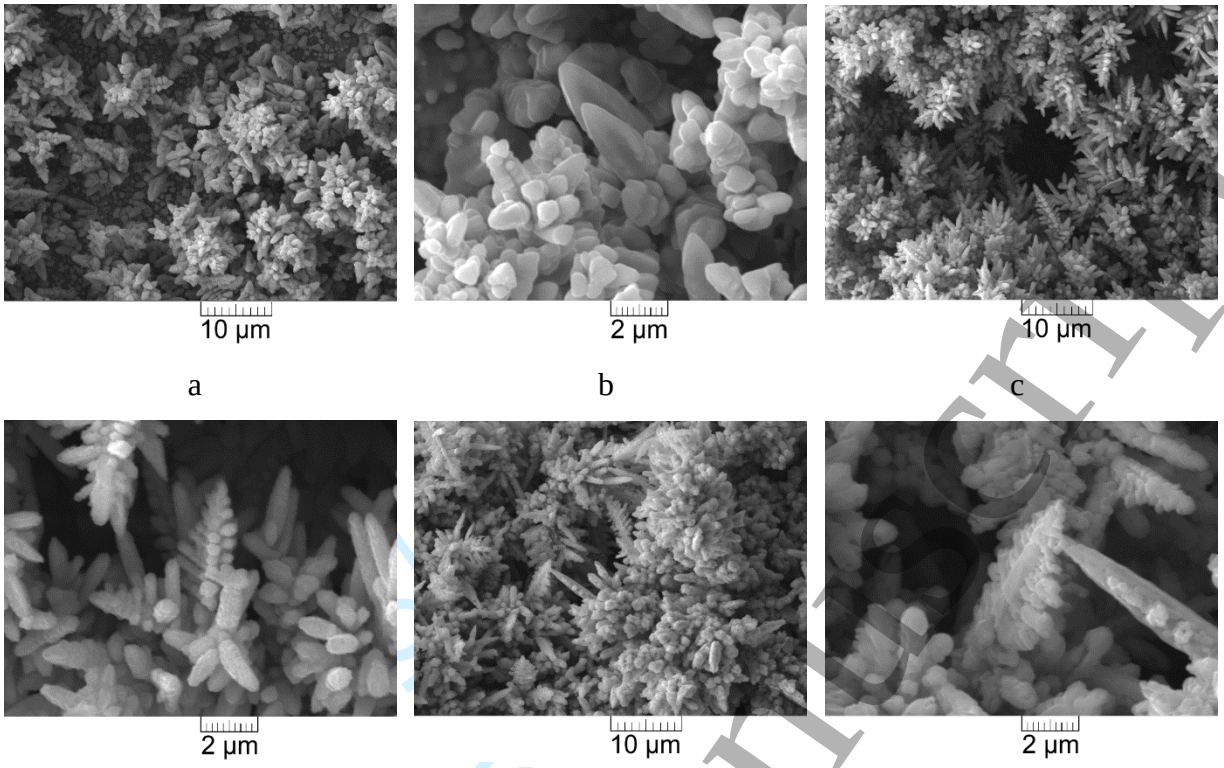

Figure 4. Morphologies of Cu deposits produced by the PO regime from 0.15 M $CuSO_4$ in 0.50 M H_2SO_4 with η_A of –1400 mV and by an addition of chloride ions of: a) and b) 5 mM, c) and d) 15 mM, and e) and f) 30 mM HCl.

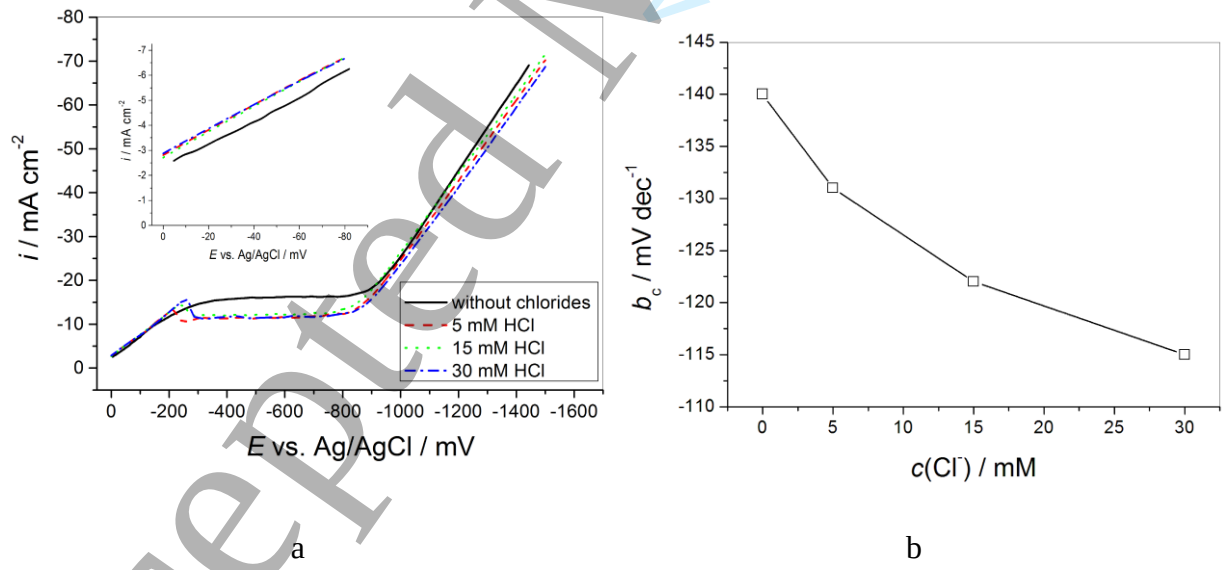

Figure 5. a) The cathodic polarization curves for copper electrodeposition from 0.15 M $CuSO_4$ in 0.50 M H_2SO_4, and with an addition of 5, 15 and 30 mM HCl, and b) the dependencies of the cathodic Tafel slopes on the concentration of chloride ions.

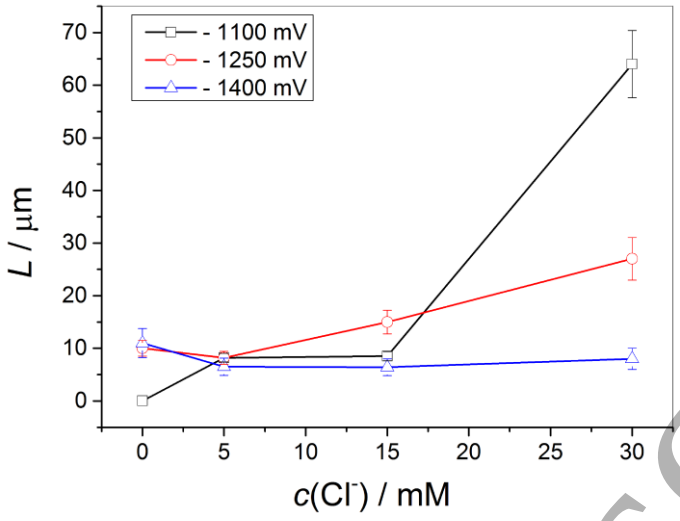

Figure 6. The dependencies of the particle size defined by a length of dendrite stalk (L) on the concentration of chloride ions obtained at the various overpotential amplitudes.

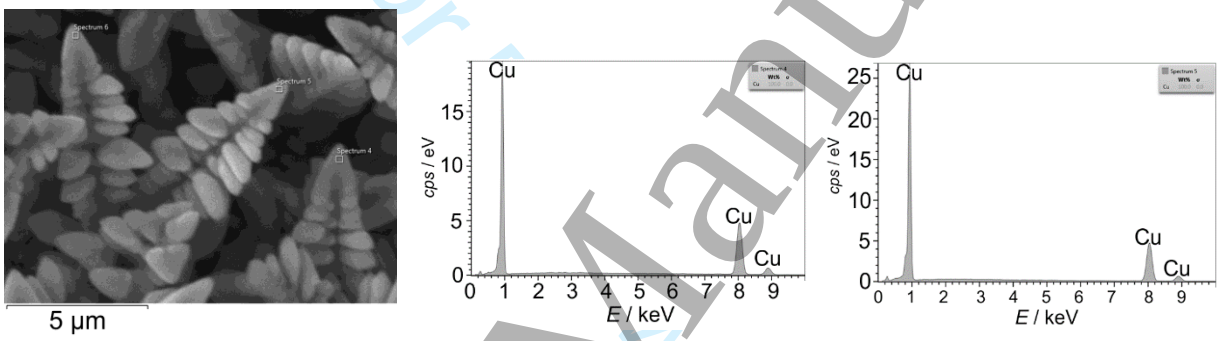

a b c

Figure 7. The SEM micrograph and EDS spectrums obtained from the corresponding parts of the Cu dendrites close to their tips.

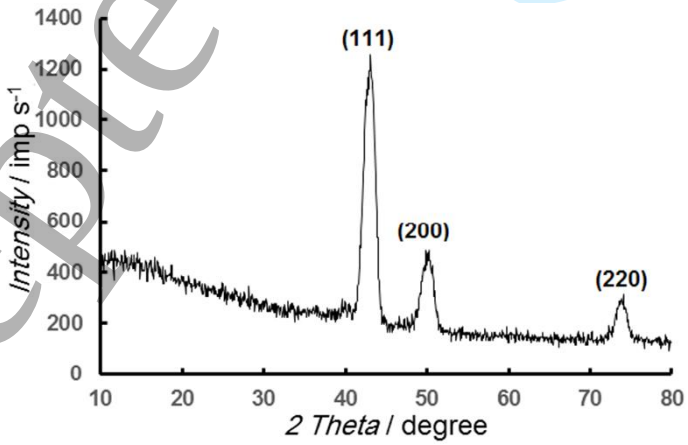

Figure 8. XRD pattern of Cu dendrites produced by the PO regime with η_A of –1250 mV and by an addition of chloride ions of 5 mM.